

## Supporting Information

### **Spatial regulation of electroplex emission by dendritic molecular engineering**

*Dan Liu, Ao Guo, Qianyi Zhang, Yingli Feng, Guimin Zhao, Daiyu Ma, Haowen Chen,  
Wei Jiang\*, Yueming Sun*

Jiangsu Province Hi-Tech Key Laboratory for Bio-Medical Research, Jiangsu Engineering Laboratory of Smart Carbon-Rich Materials and Device, School of Chemistry and Chemical Engineering, Southeast University, Nanjing, 211189, China

\* To whom correspondence should be addressed. Emails: [jiangw@seu.edu.cn](mailto:jiangw@seu.edu.cn)

## Supporting Information

### General information

All solvents and materials were used as received from commercial sources without further purification.  $^1\text{H}$  NMR spectra and  $^{13}\text{C}$  NMR were recorded on a BRUKER AMX 600 MHz and 150 MHz instrument relative to  $\text{Si}(\text{CH}_3)_4$  as internal standard. Molecular masses were determined by matrix-assisted laser desorption-ionization time-of-flight mass spectrometry (MALDI-TOF-MS) using a BRUKER DALTONICS instrument, with  $\alpha$ -cyano-hydroxycinnamic acid as a matrix. Absorption and photoluminescence emission spectra of the target compound were measured using a SHIMADZU UV-2450 spectrophotometer and a HORIBA FLUOROMAX-4 spectrophotometer, respectively. The solid PL quantum efficiency was measured with an integrating sphere. Cyclic voltammetry was performed on a CHI750C voltammetric analyzer in  $\text{CH}_2\text{Cl}_2$  solutions ( $10^{-3}$  M) (oxidation process) at a scan rate of  $100 \text{ mV s}^{-1}$  with a platinum plate as the working electrode, a silver wire as the pseudoreference electrode, and a platinum wire as the counter electrode. The supporting electrolyte was tetrabutylammonium hexafluorophosphate (0.1 M) and ferrocene was selected as the internal standard. Thermogravimetric analysis (TGA) and differential scanning calorimetry (DSC) curves were recorded with a Netzsch simultaneous thermal analyzer (STA) system (STA 409 PC) and DSC 2910 modulated calorimeter under a dry nitrogen gas flow at a heating rate of  $10 \text{ C min}^{-1}$ .

### Devices measurements and characterization

To fabricate the nondoped solution-processed OLEDs, a 40 nm-thick poly(3,4-

ethylenedioxythiophene): poly(styrenesulfonate) (PEDOT: PSS) film was firstly deposited on the pre-cleaned ITO-glass substrates and baked at 150 °C for 10 min. Then, the EML with a thickness of about 40 nm was spin-coated from a 1, 2-dichloroethane solution onto the PEDOT: PSS layer and annealed at 100 °C for 30 min to remove the residual solvent in N<sub>2</sub> atmosphere. Subsequently, a 40 nm thick TPBi were evaporated as the hole blocking and electron transporting layer. Finally, a 1 nm thick Cs<sub>2</sub>CO<sub>3</sub> and 100 nm thick Al were evaporated as the cathode. The EL spectra and CIE coordinates were measured using a PR655 spectra colorimeter. The current density-voltage and brightness-voltage curves of the devices were measured using a Keithley 2400 source meter calibrated by a silicon photodiode. All the measurements were carried out at room temperature under ambient conditions. The EQE was calculated from the brightness, current density and EL spectrum assuming a Lambertian distribution.

### **Material and synthesis**

(1) tris(4-(3-((6-(9H-carbazol-9-yl)hexyl)oxy)-9H-carbazol-9-yl)phenyl)amine (TCTA - O - CZ)

The reactants 3-((6-(9H-carbazol-9-yl)hexyl)oxy)-9H-carbazole (CZ-O-CZ) (2.63 g, 6.08 mmol), tris(4-iodophenyl)amine (3I-TPA) (1.18 g, 1.9 mmol), potassium carbonate (0.84g, 6.71 mmol), copper iodide (0.12 g, 0.63 mmol), 1, 10-phenanthroline (0.024 g, 1.19 mmol) and 40 mLDMAC solutions were placed in a 100 mL round-bottom reaction flask at 166 °C for 24 h. The reaction takes place under the protection of nitrogen. After the reaction was completed, the reaction liquid was placed to cool

down, and 150 mL of water was first added for quenching reaction near room temperature, followed by extraction operation ( $\text{CH}_2\text{Cl}_2$ , 3 times). The obtained organic layers were confluenty steamed together, and then anhydrous  $\text{Na}_2\text{SO}_4$  was added (to absorb water), filtered and dried. The coarse product was mixed with silica gel to make sand. The purification process was carried out by silica gel column, and the eluent was petroleum ether/dichloromethane. Finally, after drying in the drying box, the final product was 1.82 g white powder with a yield of 62.7%.

$^1\text{H}$  NMR (600 MHz,  $\text{DMSO-d}_6$ ,  $\delta$ ) : 8.20 (d,  $J=7.92$  Hz, 3H) , 8.13 (d,  $J=7.68$  Hz, 6H) , 7.77 (s, 3H) , 7.61 (q, 12H) , 7.51 (d,  $J=8.76$  Hz, 6H) , 7.45-7.40 (m, 12H) , 7.34 (d,  $J=8.82$  Hz, 3H) , 7.23 (t,  $J=6.84$  Hz, 3H) , 7.16 (t,  $J=7.74$  Hz, 6H) , 7.01 (dd,  $J=8.88$  Hz, 3H) , 4.39 (t,  $J=7.08$  Hz, 6H) , 4.02 (t,  $J=6.42$  Hz, 6H) , 1.84-1.79 (m, 6H) , 1.73-1.68 (m, 6H) , 1.51-1.46 (m, 6H) , 1.42-1.37 (m, 6H) . MS (MALDI-TOF) [m/z], calcd for  $\text{C}_{108}\text{H}_{93}\text{N}_7\text{O}_3$ , 1627.19; found, 1625.39. Anal. Calcd. for  $\text{C}_{114}\text{H}_{111}\text{N}_7\text{O}_3$ , C, 84.15; H, 6.88; N, 6.03; O, 2.95. Found, C, 84.04; H, 6.88; N, 6.01 °

(2) tris(4-(3,6-bis((6-(9H-carbazol-9-yl)hexyl)oxy)-9H-carbazol-9-yl)phenyl)amine (TCTA - O - 2CZ)

The synthesis steps of TCTA-O-2CZ were basically the same as those of TCTA-O-CZ, and the final product was white powder with a yield of 51.4%.

$^1\text{H}$  NMR (600 MHz,  $\text{DMSO-d}_6$ ,  $\delta$ ) : 8.12 (d,  $J=7.74$  Hz, 12H) , 7.76 (s, 6H) , 7.58 (d,  $J=8.22$  Hz, 18H) , 7.47 (d,  $J=8.28$  Hz, 6H) , 7.41 (t,  $J=7.98$  Hz, 12H) , 7.32 (d,  $J=9.18$  Hz, 6H) , 7.16 (t,  $J=7.44$  Hz, 12H) , 6.98 (d,  $J=9.54$  Hz, 6H) ,

4.40 (t, J=7.08 Hz, 12H) , 4.01 (m, 12H) , 1.82-1.71 (m, 24H) , 1.49-1.38 (m, 24H) . MS (MALDI-TOF) [m/z], calcd for C<sub>162</sub>H<sub>150</sub>N<sub>10</sub>O<sub>6</sub>, 2468.36; found, 2467.15. Anal. Calcd. for C<sub>162</sub>H<sub>150</sub>N<sub>10</sub>O<sub>6</sub>, C, 83.21; H, 7.23; N, 5.67; O, 3.89. Found, C, 83.11; H, 7.23; N, 5.65.

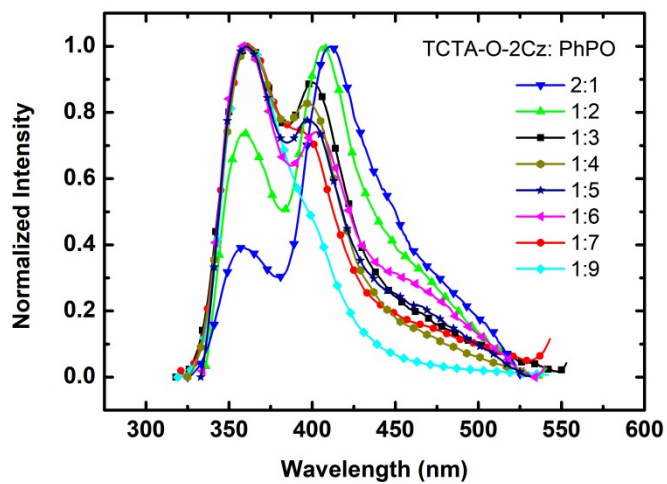


Figure S1 The PL spectra of TCTA-O-2CZ: PhPO blending films with different molar ratios of 2:1, 1:2, 1:3, 1:4, 1:5, 1:6, 1:7, 1:9.

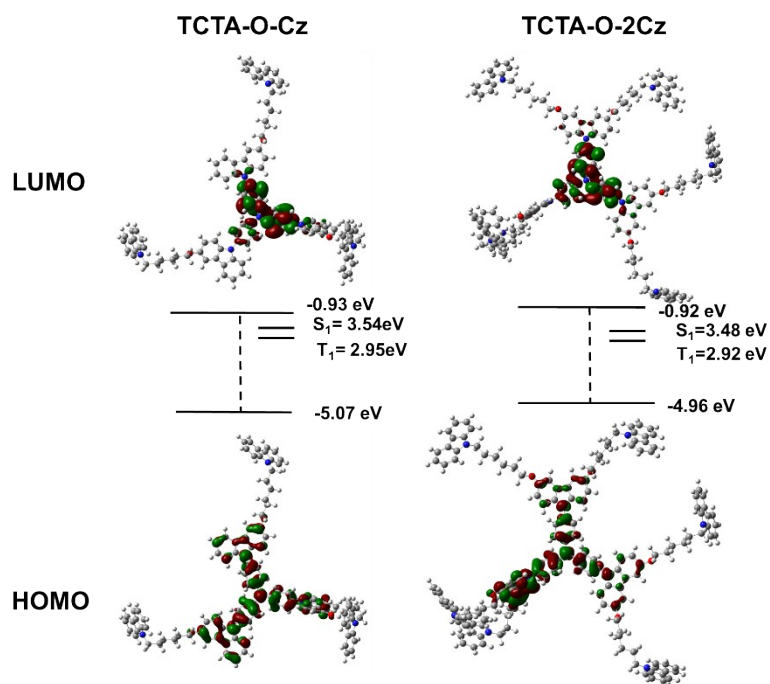


Figure S2. The optimization of frontier molecular orbital electron cloud distribution and calculated values of HOMO/LUMO and  $S_1/T_1$  energy.

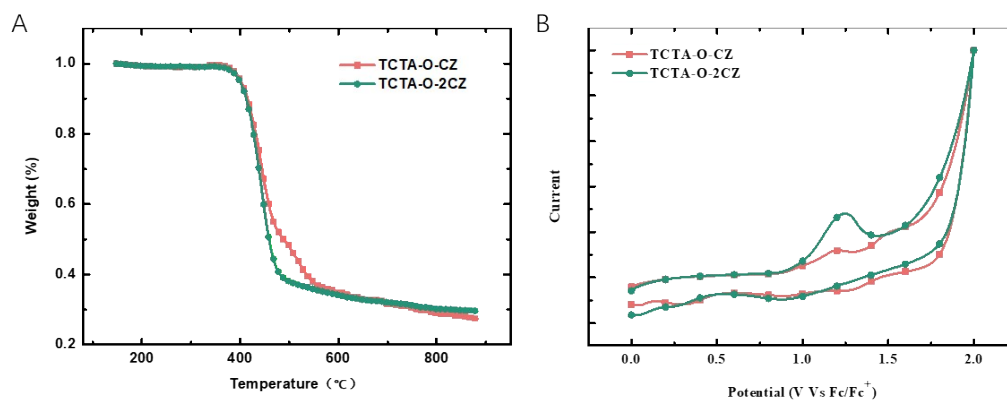


Figure S3. (A) TGA curve of TCTA-O-CZ and TCTA-O-2CZ recorded at a heating rate of  $10\text{ }^\circ\text{C min}^{-1}$ . (B) CV curves of TCTA-O-CZ and TCTA-O-2CZ in  $\text{CH}_2\text{Cl}_2$  for oxidation scan.

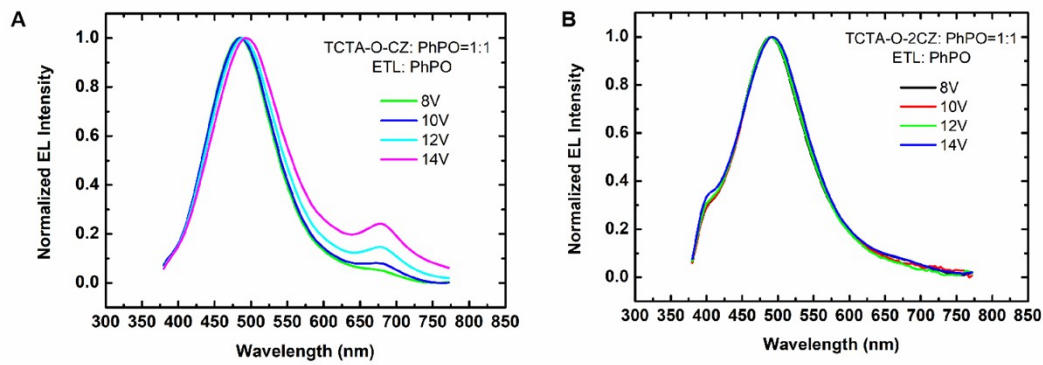


Figure S4 The EL spectra of Device F and G (ITO/PEDOT:PSS/TCTA-O-CZ: PhPO (Device F) or TCTA-O-2CZ: PhPO (Device G)/PhPO/Cs<sub>2</sub>CO<sub>3</sub>/Al)

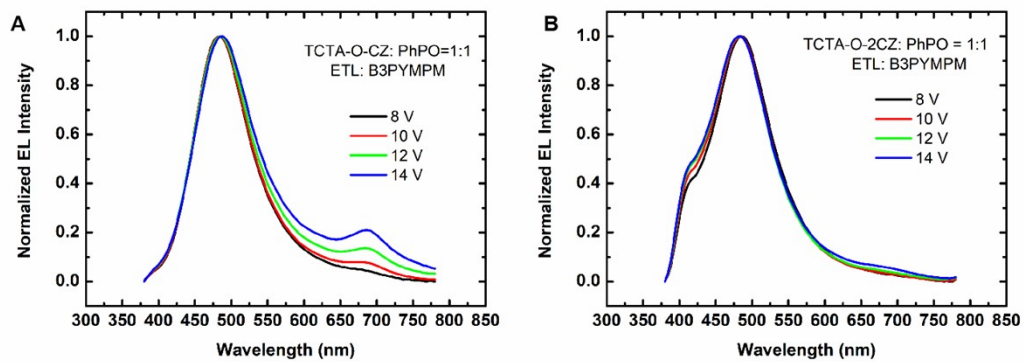


Figure S5 The EL spectra of Device H and I (ITO/PEDOT:PSS/TCTA-O-CZ: PhPO (Device F) or TCTA-O-2CZ: PhPO (Device G)/B3PYMPM/Cs<sub>2</sub>CO<sub>3</sub>/Al)

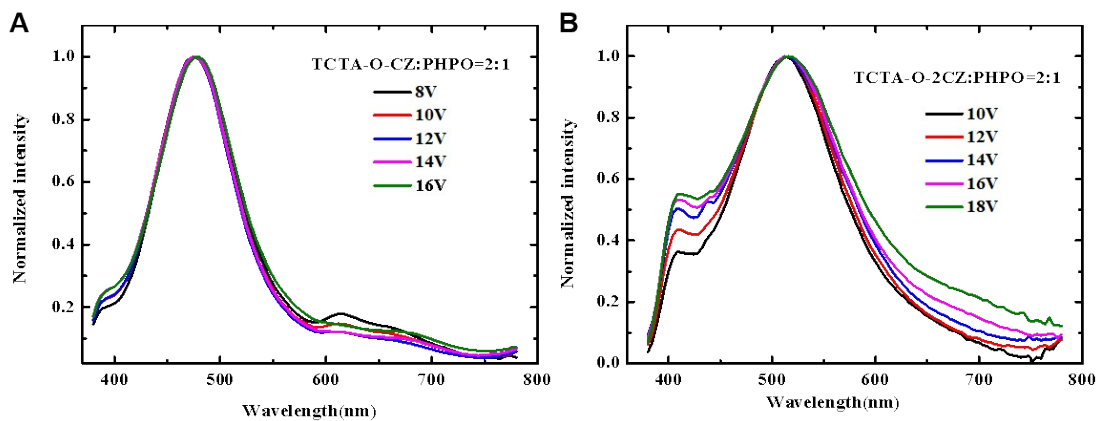


Figure S6. The EL spectra of 2:1 (a) TCTA-O-CZ:PhPO, (b) TCTA-O-2CZ:PhPO at different voltages.

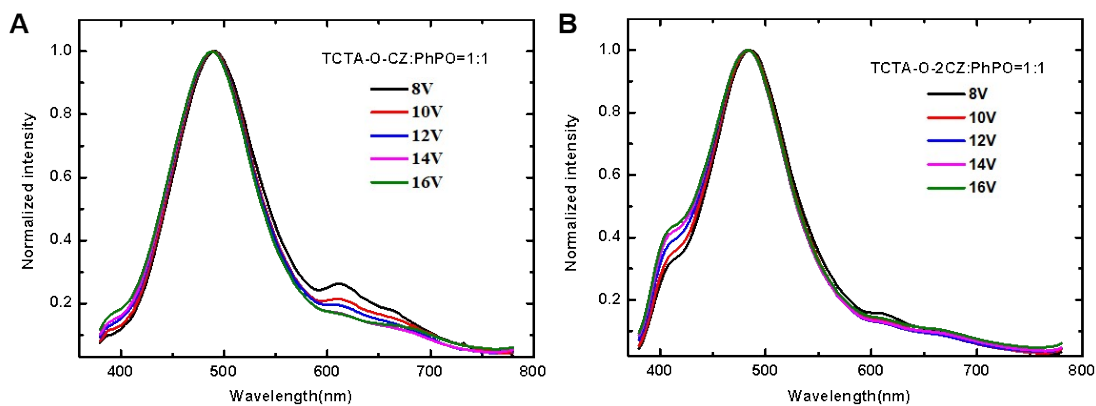


Figure S7. The EL spectra of 1:1 (a) TCTA-O-CZ:PhPO, (b) TCTA-O-2CZ:PhPO at different voltages.

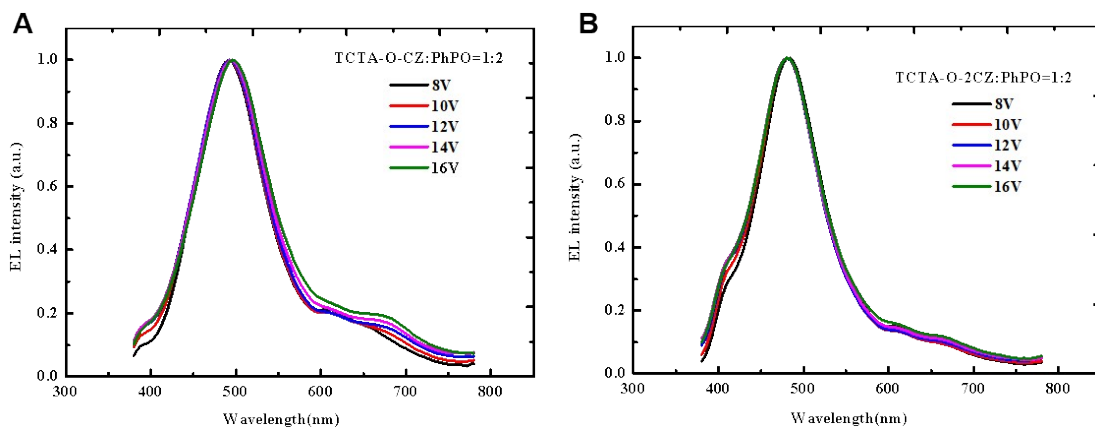


Figure S8. The EL spectra of 1:2 (a) TCTA-O-CZ:PhPO, (b) TCTA-O-2CZ:PhPO at different voltages.

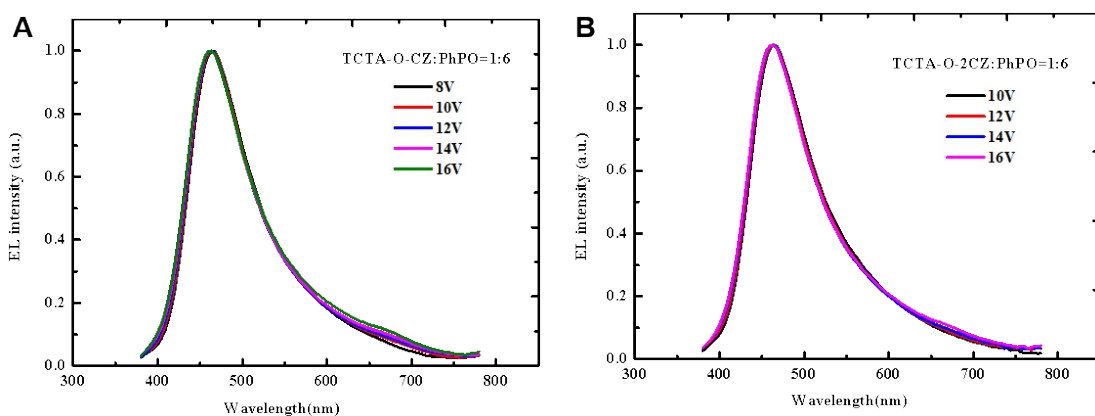


Figure S9. The EL spectra of 1:6 (a) TCTA-O-CZ:PhPO, (b) TCTA-O-2CZ:PhPO at different voltages.



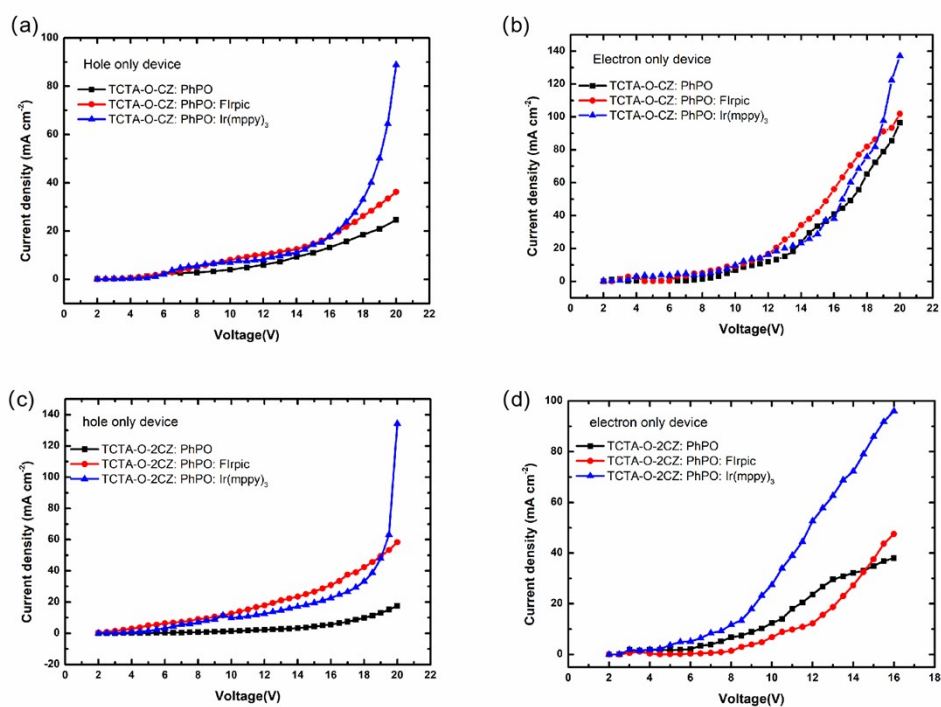


Figure S10 Current density-voltage (J-V)characteristics o carrier-only devices: (a) hole only and (b) electron only devices.